Arch. Mech., **55**, 5–6, pp. 519–530, Warszawa 2003

# Pseudoviscoelastic behavior of TiNi shape memory alloys under stress-controlled subloop loadings

H. TOBUSHI[(1)], M. ENDO[(2)], T. IKAWA[(1)] D. SHIMADA[(1)]

[(1)] *Department of Mechanical Engineering*
*Aichi Institute of Technology*
*1247 Yachigusa, Yagusa-cho, Toyota 470-0392 Japan*

[(2)] *Toshiba Ceramics Co., Ltd.*
*Nishi-shinjuku 7-5-25, Shinjuku-ku, Tokyo 160-0023 Japan*

THE SUPERELASTIC BEHAVIOR of TiNi shape memory alloy under various subloop loadings were investigated. The results obtained can be summarized as follows. (1) In the case of subloop loading under strain-controlled conditions, the reloading curve passes through the unloading-start point. In the case of stress-controlled conditions, the return-point memory does not appear. (2) In the case of subloop loading under stress-controlled conditions, strain increases under constant stress in the loading process and decreases in the unloading process. (3) In the case of subloop loading under stress-controlled conditions, stress decreases under constant strain in the loading process and increases in the unloading process. (4) The above-mentioned behavior concerning the return-point memory and the pseudoviscoelastic behavior similar to creep and stress relaxation, appear according to the martensitic transformation and the reverse transformation based on the variation in stress and temperature.

**Key words:** Shape memory alloy, superelasticity, subloop, return-point memory, creep, stress relaxation, titanium-nickel alloy, stress control.

## 1. Introduction

IN SHAPE MEMORY alloys (SMAs), the shape memory effect and superelastic characteristics appear based on the martensitic transformation (MT) [1–7]. In practical applications of SMAs, SMA elements are subjected to various thermomechanical loadings. In order to design SMA elements, the thermomechanical properties of SMAs are important.

Recently it has been reported that the deformation behavior under subloop loadings is different between the strain-controlled condition and the stress-controlled condition [8]. Although the return-point memory appears in the subloop loading under the strain-controlled condition, it does not appear under the stress-controlled condition. In the case of the stress-controlled condition, temperature increases due to the MT in the loading process and decreases due to the reverse transformation in the unloading process. Both the stress and strain vary based on these variations in temperature, and therefore the return-point memory does not appear in the case of stress-controlled conditions [9]. Recently it has been also reported that creep deformation and stress relaxation appear in SMAs under the subloop loadings [10].

In the present study, the superelastic behavior of TiNi SMAs under various loading conditions are investigated experimentally. The conditions to cause the return-point memory are discussed. The pseudoviscoelastic behavior of creep deformation and stress relaxation under the subloop loadings with the stress-controlled condition is also discussed.

## 2. Experimental methods

### 2.1. Materials and specimens

The material tested was a rectilinear Ti–55.4wt%Ni SMA wire, 0.75 mm in diameter, produced by Furukawa Electric Co. Its straightness was shape-memorized through shape-memory processing. This was done by holding the wire rectilinear at 673 K for 60 min followed by cooling in the furnace. The reverse-transformation finish temperature $A_f$ was about 323 K.

### 2.2. Experimental apparatus

The SMA testing machine was used. The machine was composed of the tensile machine and the heating-cooling device. Displacement was measured by an extensometer with gauge length of 20 mm. Temperature was measured by a thermocouple, 0.1 mm in diameter, which was pressed on the specimen at the central part of the gauge length.

### 2.3. Experimental procedure

In order to investigate the superelastic properties of the material, the following five kinds of thermomechanical tension tests under various loading conditions were carried out by keeping the ambient temperature $T = 353$ K above $A_f$ constant. Stress and strain were treated in terms of nominal stress and nominal strain, respectively. Therefore the stress-controlled and strain-controlled conditions mean the load-controlled and displacement-controlled conditions, respectively.

1. *Full-loop loading under constant strain rate and stress rate*
   In the tension test, the full-loop loading and unloading were applied under constant strain rate $\dot{\varepsilon}$ and stress rate $\dot{\sigma}$. The MT completes in the loading process and the reverse transformation completes in the unloading process.

2. *Subloop loading under constant strain rate*
   Strain rate $\dot{\varepsilon}$ was kept constant during the loading and unloading processes. In the loading process, it was unloaded before the completion of the MT. In the unloading process, it was reloaded before the completion of the reverse transformation. The subloop-loading processes were repeated.

3. *Subloop loading under constant stress rate*
   Stress rate $\dot{\sigma}$ was kept constant during the subloop-loading and unloading processes. The subloop-loading processes were repeated.

4. *Subloop loading under constant stress*
   Stress was kept constant during the MT in the loading process and during the reverse transformation in the unloading process for a certain duration. Variation in strain was observed under constant stress.

5. *Subloop loading under constant strain*
   Strain was kept constant during the MT in the loading process and during the reverse transformation in the unloading process for a certain duration. Variation in stress was observed under constant strain.

## 3. Experimental results and discussion

### 3.1. Full-loop superelastic behavior under constant strain rate and stress rate

The stress-strain curves obtained by the tension test under constant strain rate $\dot{\varepsilon}$ and stress rate $\dot{\sigma}$ are shown in Fig. 1. As it can be seen, in the case of $\dot{\varepsilon} = 1\%/\text{min}$, the overshoot occurs at the MT-start point $M_S$ in the loading process and the MT progresses in the region of the upper stress plateau till the MT-end point $M_F$. In the unloading process, the undershoot occurs at the reverse-transformation start point $A_S$ and the reverse transformation progresses in the region of the lower stress plateau till the end point $A_F$.

On the other hand, in the case of constant stress rate $\dot{\sigma}$, the overshoot at the point $M_S$ and the undershoot at the point $A_S$ do not appear. Both the MT and the reverse transformation progress with a certain slope of the curve between the points $M_s$ and $M_f$ and between the points $A_s$ and $A_f$, respectively. The larger is the stress rate, the more steep will be the slope of the curve. The stress-strain curve under constant stress rate is similar to that under high strain rate [11, 12]. If the strain rate is high, the overshoot and undershoot do not appear, and temperature increases due to the MT in the loading process and decreases due to the reverse transformation in the unloading process. The variation in

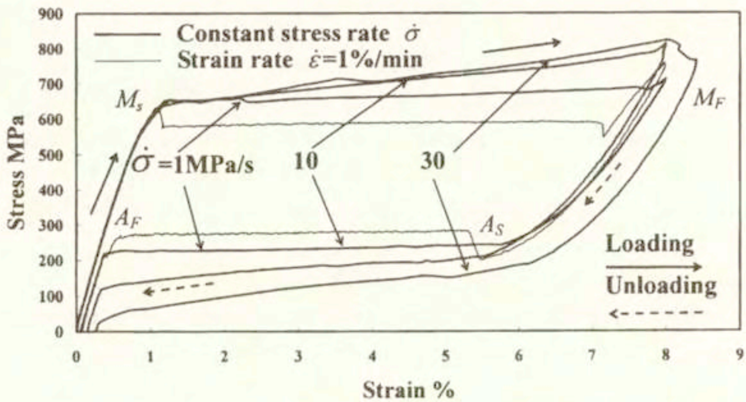


FIG. 1. Stress-strain curves for full-loop loading under constant strain rate $\dot{\varepsilon}$ and stress rate $\dot{\sigma}$.

temperature under constant stress rate is similar to that under high strain rate.

### 3.2. Subloop superelastic behavior under strain-controlled condition

The stress-strain curves obtained by the subloop loading test under constant strain rate $\dot{\varepsilon} = 1\%/\text{min}$ are shown in Fig. 2. In the test, the process ($A_i$, $B_i$ and $C_i$) corresponds to unloading and the process ($C_i$, $D_i$ and $A_{i+1}$) to reloading. The process ($A_i$, $B_i$) and the process ($C_i$, $D_i$) are elastic. The reverse transformation appears in the process ($B_i$, $C_i$) and the MT appears in the process ($D_i$, $A_{i+1}$). The MT stress decreases under cyclic deformation [13]. Therefore the MT stress plateau during the reloading process ($D_i$, $A_{i+1}$) decreases with an increase in the number of cycles $N$. The reloading curve ($C_i$, $D_i$ and $A_{i+1}$) passes through the unloading-start point $A_i$. Therefore the return-point memory is observed in the case of the strain-controlled condition.

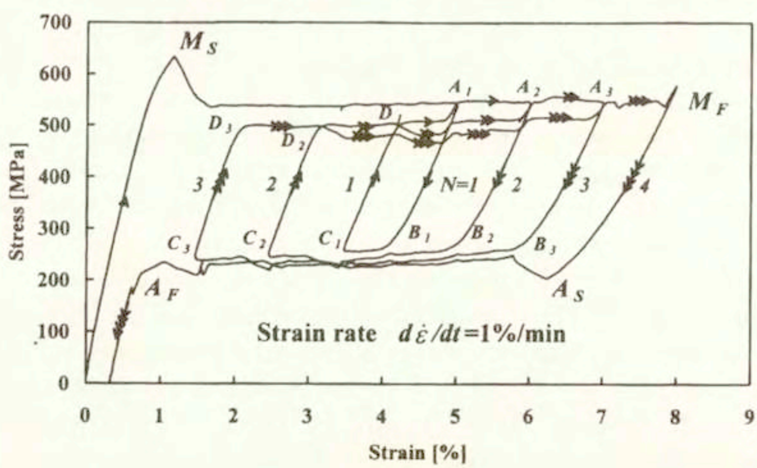


FIG. 2. Stress-strain curves for subloop loading under constant strain rate $\dot{\varepsilon}$.

### 3.3. Subloop superelastic behavior under stress-controlled condition

1. *Stress-strain curve*

The stress-strain curves obtained by the subloop loading test under constant stress rate $\dot{\sigma}$ are shown in Fig. 3. As it can be seen, strain increases in the early stage of unloading ($A_i$, $B_i$) and decreases in the early stage of reloading ($D_i$, $E_i$). The variation in strain is lager under low-stress rate.

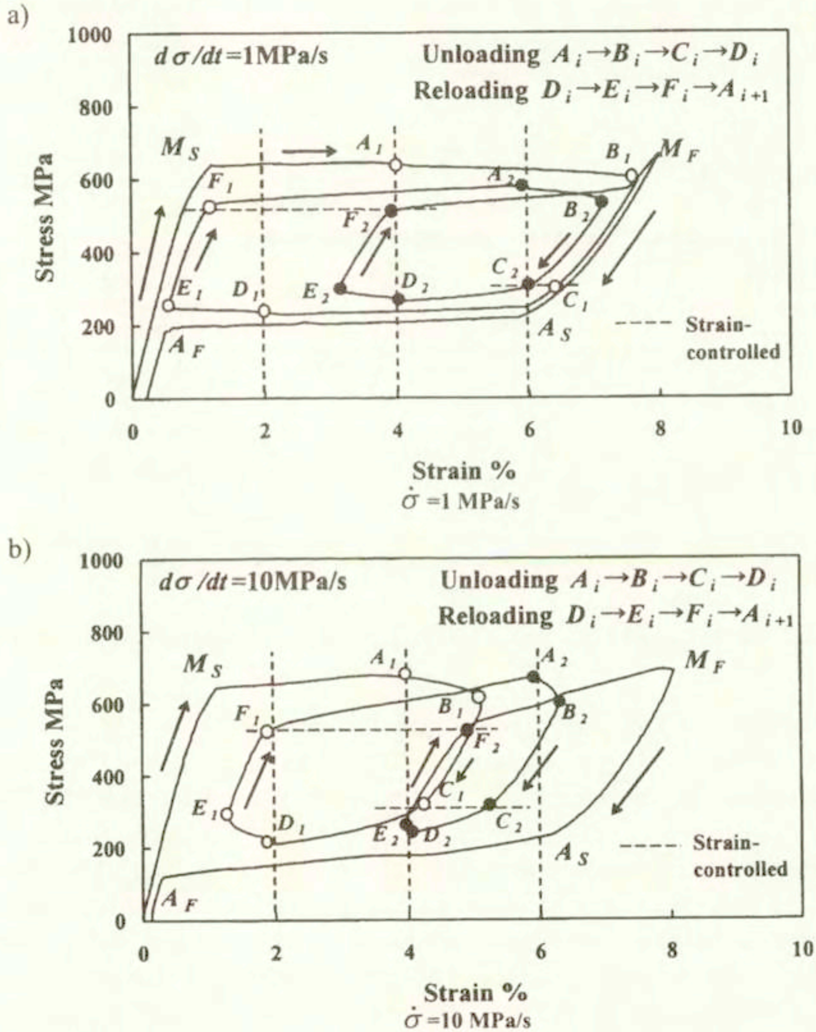


FIG. 3. Stress-strain curves for subloop loading under constant stress rate $\dot{\sigma}$.

These strain behaviors are quite different from those under constant strain rate observed in Fig. 2. In the reloading process, the stress-strain curve does not pass through the unloading-start point $A_i$. Therefore the return-point memory which is observed under the strain-controlled condition does not appear under the stress-controlled condition.

2. *Variation in temperature*

The variation in temperature obtained during the subloop loading under $\dot{\sigma} = 1$ MPa/s is shown in Fig. 4. In Fig. 4, the variation in temperature is shown as a function of the accumulated strain path $\Sigma|\Delta L/L|$. As it can be seen, temperature increases due to the MT in the loading process and decreases in the early stage of unloading ($A_i$, $B_i$). Temperature decreases due to the reverse transformation in the unloading process and increases in the early stage of reloading ($D_i$, $E_i$).

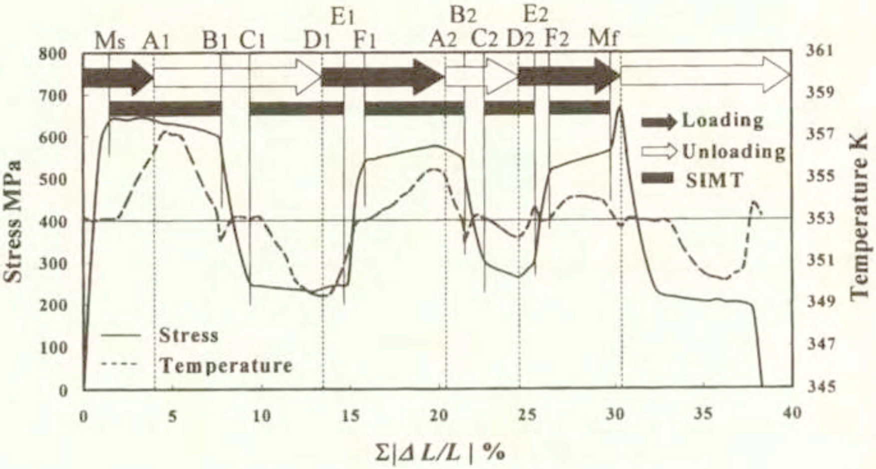


FIG. 4. Variation in temperature for subloop loading under constant stress rate $\dot{\sigma}=1$ MPa/s.

3. *Condition for progress of phase transformation*

The condition for the progress of the MT and the reverse transformation is governed by the kinetics of the phase transformation [14, 15]. The condition for the progress of the phase transformation under subloop loadings is shown on the stress-temperature phase diagram in Fig. 5 [9]. The conditions for the start and finish of the MT and the reverse transformation are expressed by the transformation lines $M_S$, $M_F$, $A_S$ and $A_F$, respectively. Each transformation progresses in the transformation strip between the start line and the finish line. As it can be seen, the MT progresses if the state of stress and temperature varies to the direction in which the volume fraction $\xi$ of the $M$-phase increases. The reverse transformation progresses if the state varies to the direction in which $\xi$ decreases. Based on this consideration, the MT must progress in the early stage of unloading ($A_i$, $B_i$) under constant $\dot{\sigma}$ and strain increases as observed in Fig. 3. The reverse transformation must progress in the early stage of reloading ($D_i$, $E_i$) and strain decreases as observed in Fig. 3.

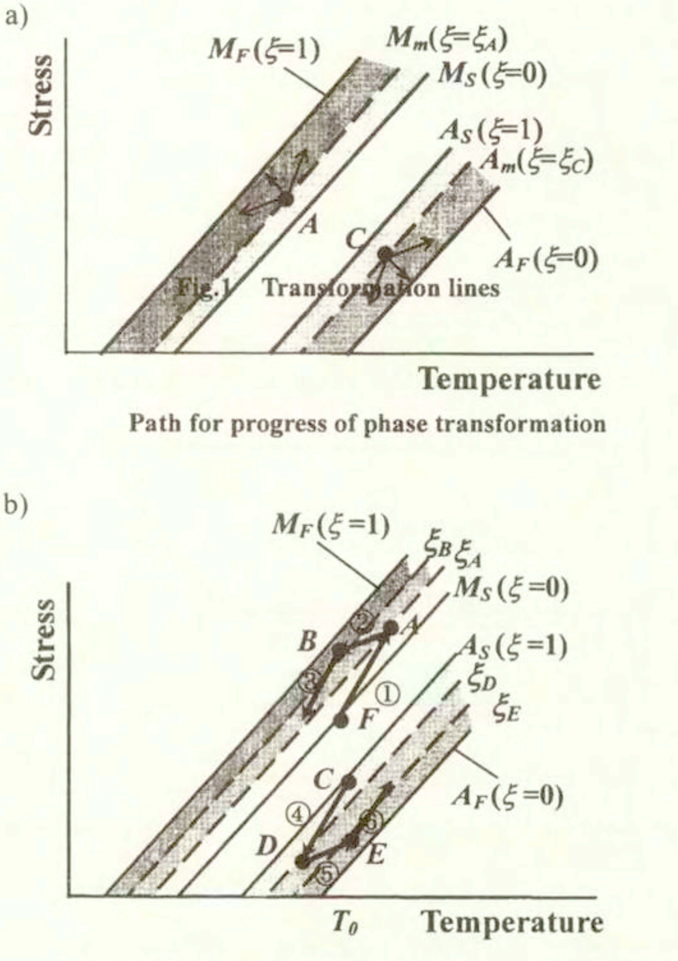


FIG. 5. Conditions for progress of the MT and the reverse transformation under subloop loadings: a) Path for progress of phase transformation, b) Path for progress and stop of phase transformation.

#### 3.4. Strain behavior under constant stress

The stress-strain curve obtained by the subloop loading test under constant stress is shown in Fig. 6. In the loading process ($O$, $A$) and the unloading process ($B, C$), stress rate was 1 MPa/s. Stress was kept constant during the process

$(A, M_F)$ following the point $A$ and during the process $(C, A_F)$ following the point $C$. The condition of constant stress will correspond to very low stress rate. Therefore, as observed in Figs. 3, 4 and 5, the MT progresses under low stress rate or constant stress due to decrease in temperature, resulting in increase in strain. The reverse transformation also progresses under constant stress due to increase in temperature, resulting in decrease in strain. The increase in strain under constant stress is similar to creep deformation and the decrease in strain under constant stress is similar to creep recovery after unloading which appear in the viscoelastic material. These creep and creep recovery in SMA must appear owing to the MT and the reverse transformation, respectively, based on the variation in temperature.

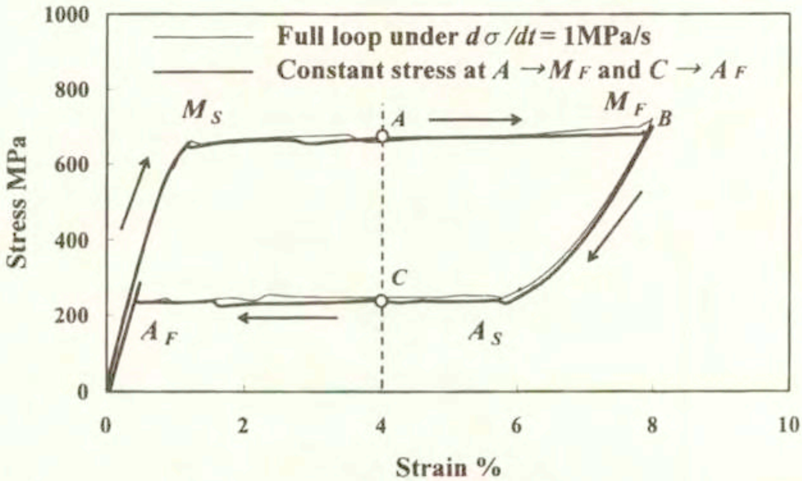


FIG. 6. Stress-strain curves for subloop loading under constant stress during loading and unloading.

As observed above, temperature varies due to the phase transformation during loading and unloading, and temperature returns to the ambient temperature with lapse of time under constant stress, resulting in variation in strain. In order to confirm the strain behavior during variation in temperature under constant stress, the heating-cooling test under constant stress was carried out. The relationship between strain and temperature obtained by the test is shown in Fig. 7. In the test, at first, strain $\varepsilon_0 = 4\%$ at the point $A$ was applied at temperature $T^\circ = 333$ K. Following the loading to the point $A$ and keeping stress $\sigma_0 = 460$ MPa at the point $A$ constant, the specimen was cooled down to $T_l = 303$ K which was followed by heating up to $T_h = 393$ K. The heating and cooling under constant stress were repeated twice. As it can be seen in Fig. 7, strain decreases due to the reverse transformation between $A_S$ and $A_F$ in the heating process. In the cooling process, strain increases due to the MT between $M_S$ and $M_F$. Therefore, it is important to note that, even if the ambient temperature is constant in applications of SMAs, creep and creep recovery must appear if the temperature varies based on the phase transformation in the subloop loadings.

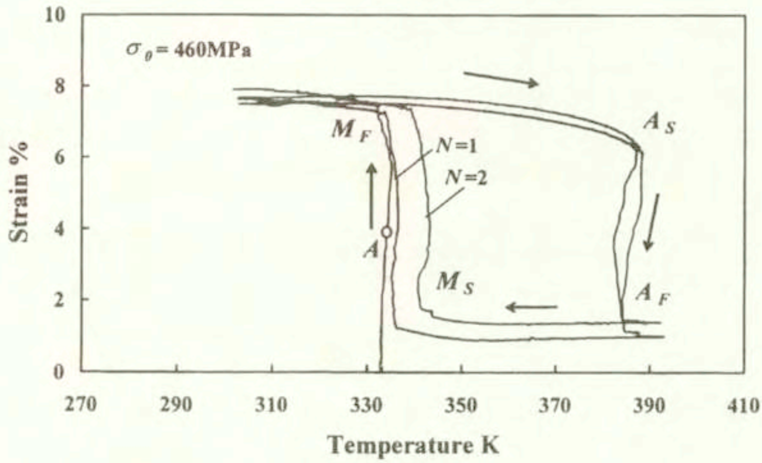


FIG. 7. Variation in strain during heating and cooling under constant stress.

### 3.5. Stress behavior under constant strain

The stress-strain curve obtained by the subloop loading test under constant strain is shown in Fig. 8. In the loading and unloading processes, stress rate was 30 MPa/s. Strain was kept constant for 10 min during the loading process $(A_i, B_i)$ and during the unloading process $(C_i, D_i)$. As it can be seen in Fig. 8, stress decreases under constant strain during $(A_i, B_i)$ and increases during $(C_i, D_i)$. The decrease in stress and the increase in stress stop on the upper stress plateau and on the lower stress plateau of the stress-strain curve under low strain rate, respectively.

The variations in stress and temperature during the first step of the subloop loading $(O, M_S, A_1$ and $B_1)$ are shown in Fig. 9. In the test, stress rate was constant during loading $(O$, $M_S$ and $A_1)$ and strain was kept constant during $(A_1, B_1)$. As it can be seen in Fig. 9, temperature increases due to the MT during loading $(M_S, A_1)$. Both the stress and temperature decrease markedly just after keeping the strain constant at the point $A_1$ and remain constant thereafter till the point $B_1$. Although temperature varies due to the MT in the early stage under constant strain, temperature approaches the ambient temperature after the early stage. The decrease in stress under constant strain is similar to stress relaxation, and the increase in stress under constant strain is similar to stress recovery after unloading which appear in the viscoelastic material. These stress relaxation and stress recovery must appear owing to the MT and the reverse transformation, respectively, based on the variation in temperature.

In the experiments of the present study, temperature was controlled to keep the ambient temperature constant. Therefore the variation in temperature of the material depends on the heating and cooling conditions. This means that the variations in stress and strain which appear based on the MT due to the variation in temperature, depend on the size of the SMA elements and the conditions of heat transfer between the SMA elements and atmosphere. Therefore, in order to design the SMA elements, this pseudoelastic behavior must be taken into account in the case of the stress-controlled subloop loadings.

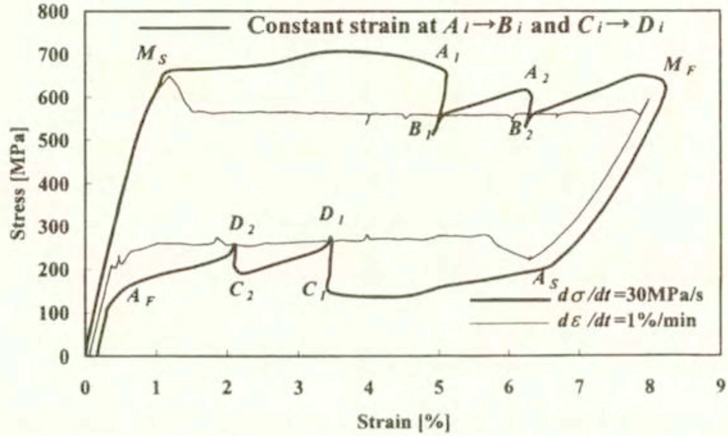


FIG. 8. Stress-strain curves for subloop loading under constant strain during loading and unloading.

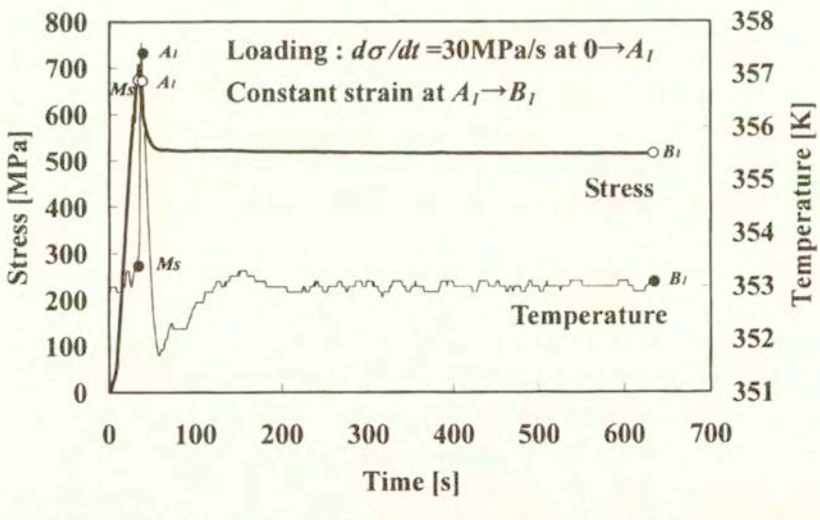


FIG. 9. Variations in stress and temperature during subloop loading with constant strain.

## 4. Conclusions

The superelastic behavior of TiNi SMA under various subloop loadings has been investigated. The results obtained can be summarized as follows.

1. In the case of subloop loading under strain-controlled conditions, the reloading curve passeses through the unloading-start point. In the case of stress-controlled conditions, the return-point memory does not appear.
2. In the case of subloop loading under stress-controlled conditions, strain increases under constant stress in the loading process and decreases in the unloading process.
3. In the case of subloop loading under stress-controlled conditions, stress decreases under constant strain in the loading process and increases in the unloading process.
4. The above-mentioned behavior concerning the return-point memory and the pseudoviscoelastic behaviors similar to creep and stress relaxation appears according to the MT and the reverse transformation based on the variation in stress and temperature.

## Acknowledgments

The experimental work of this study was carried out with the assistance of the students in Aichi Institute of Technology, to whom the authors express their gratitude. The authors are also grateful to the Scientific Research (C) in Grants-in-Aid for Scientific Research by the Japan Society for Promotion of Science for financial support.

## References

1. H. FUNAKUBO [Ed.], *Shape memory alloys*, Gordon and Breach Science Pub., 1987.
2. T. W. DUERIG, K. N. MELTON, D. STOCKEL and C. M. WAYMAN [Eds.], *Engineering aspects of shape memory alloys*, Butterworth-Heinemann, 1990.
3. K. OTUKA and C. M. WAYMAN [Eds.], *Shape memory materials*, Cambridge University Press, 1998.
4. T. SABURI [Ed.], *Shape memory materials*, Trans Tech Pub., 2000.
5. B. BRANIECKI and K. TANAKA [Eds.], *Testing and modelling the behaviour of shape memory alloys*, Arch. Mech., **51**, 6, 647–911] 1999.
6. Y. Y. CHU and L. C. ZHAO [Eds.], *Shape memory materials and its applications*, Trans. Tech. Pub., 2002.
7. Q. P. SUN [Ed.], *IUTAM Symposium on mechanics of martensitic phase transformation in solids*, Kluwer Academic Pub., 2002.

8. G. SOCHA, B. RANIECKI and S. MIYAZAKI, *Influence of control parameters on inhomogeneity and the deformation behavior of Ti-51.0at%Ni SMA undergoing martensitic phase transformation at pure tension*, 33rd Solid Mechanics Conference, 369–370, 2000.

9. H. TOBUSHI, K. OKUMURA, M. ENDO and K. TANAKA, *Deformation behavior of TiNi shape-memory alloy under strain- or stress-controlled conditions*, Arch. Mech., **54**, 1, 75–91, 2002.

10. D. HELM and P. HAUPT, *Termomechanical behavior of shape memory alloys*, Smart Structures and Materials 2001, Proc. of SPIE, **4333**, 302–313, 2001.

11. S. P. GADAJ, W. K. NOWACKI and H. TOBUSHI, *Temperature evolution during tensile test of TiNi shape memory alloy*, Arch. Mech., **51**, 6, 649–663, 1999.

12. H. TOBUSHI, K. TANAKA, Y. SHIMENO, W. K. NOWACKI and S. P. GADAJ, *Influence of strain rate on superelastic behaviour of TiNi shape memory alloy*, Proc. Instn. Mech. Engrs., **213**, Part L., 93–102, 1999.

13. H. TOBUSHI, S. YAMADA, T. HACHISUKA, A. IKAI and K. TANAKA, *Thermomechanical properties due to martensitic and R-phase transformation of TiNi shape memory alloy subjected to cyclic loadings*, Smart Mater. Struct., **5**, 788–795, 1996.

14. K. TANAKA, S. KOBAYASHI and Y. SATO, *Thermomechanics of transformation pseudoelasticity and shape memory effect in alloys*, Inter. J. Plasticity, **2**, 59–72, 1986.

15. K. TANAKA, *A thermomechanical sketch of shape memory effets: one-dimensional tensile behavior*, Res Mechanica, **18**, 251–263, 1986.

*Received December 2, 2002.*